Parity Nonconservation in Atomic Thallium

Persis S. Drell and Eugene D. Commins
Physics Department, University of California, Berkeley, California 94720, and Materials and Molecular Research Division, Lawrence Berkeley Laboratory, Berkeley, California 94720
(Received 29 May 1984)

We present new measurements of parity conservation in the 293-nm transition in atomic $^{205}_{81}$Tl. Linearly polarized 293-nm photons, polarization $\hat{\epsilon}$, are absorbed by $6^2P_{1/2}$ atoms in crossed electric and magnetic fields. The transition probability for each Zeeman component contains a term proportional to $\hat{\epsilon}\cdot\vec{B}\hat{\epsilon}\cdot\vec{E}\times\vec{B}$ arising from interference between the Stark $E1$ amplitude βE and the parity-nonconserving $E1$ amplitude $\mathcal{E}_p$. Our result, $[\mathrm{Im}\,\mathcal{E}_p/\beta]_{\mathrm{expt}} = -1.73\pm0.33$ mV/cm, is compared with estimates based on the standard electroweak model.

PACS numbers: 11.30.Er, 12.30.Cx, 32.90.+a

According to the standard $SU(2)\times U(1)$ electroweak model, parity nonconservation (PNC) occurs in an atom because of interference between electromagnetic and neutral weak amplitudes, and is detected most readily in heavy atoms.[1] Observations of PNC by optical rotation have been reported[2,3] in $_{83}$Bi and $_{82}$Pb. Stark interference experiments have been carried out with the $6S_{1/2}\rightarrow 7S_{1/2}$ transition in $_{55}$Cs(539 nm),[4] and the $6P_{1/2}\rightarrow 7P_{1/2}$ transition in $_{81}$Tl(293 nm).[5] The present experiment on Tl employs a different method and achieves much better precision than the previous result.

The $6P_{1/2}\rightarrow 7P_{1/2}$ Tl transition (see Fig. 1) is forbidden $M1$ with measured amplitude[6] $M = (-2.1\pm0.3)\times10^{-5}\mu_0$ where $\mu_0 = |e\hbar/2m_ec|$. PNC causes the $6P_{1/2}$ and $7P_{1/2}$ states to be mixed with $^2S_{1/2}$ states. Thus the transition amplitude also contains an $E1$ component $\mathcal{E}_p = -\langle 7P_{1/2},m_J=\frac{1}{2}|E1|6P_{1/2},m_J=\frac{1}{2}\rangle$ where $|6P_{1/2}\rangle$, $|7P_{1/2}\rangle$ are eigenstates perturbed by the effective Hamiltonian for Z^0 exchange. In the presence of an external electric field E the $P_{1/2}$ states are mixed by the Stark effect with the $S_{1/2}$ and $D_{3/2}$ states. The transition amplitude then acquires a Stark-induced $E1$ component in addition. For photon linear polarization $\hat{\epsilon}\perp\vec{E}$ (as in this work), the Stark amplitude is βE where[7] $\beta E|_{\mathrm{theor}} = (1.64\ \pm0.25)\times10^{-5}\mu_0\ E$(V/cm).

In the present experiment the $6P_{1/2}\rightarrow 7P_{1/2}$ transition occurs by absorption of linearly polarized 293-nm light in crossed electric (E) and magnetic (B) fields,[8] and is detected by observation of the 535-nm fluorescence accompanying the decay $(7P_{1/2}\rightarrow)\ 7S_{1/2}\rightarrow 6P_{3/2}$ (see Fig. 1). The magnetic field ($B = 3.2$ kG) is chosen large enough so that individual Zeeman components are resolved. For the relative orientation of $\hat{\epsilon}$ and $\vec{E}$ chosen here, M does not interfere with $\mathcal{E}_p$ or βE, but there is interference between $\mathcal{E}_p$ and βE. The absorption transition probability for each Zeeman component contains a pseudoscalar term proportional to $\hat{\epsilon}\cdot\vec{B}\hat{\epsilon}\cdot\vec{E}\times\vec{B}$. The experiment is carried out by measuring an asymmetry in the 535-nm intensity when $\vec{E}$ or θ (the angle between $\hat{\epsilon}$ and $\vec{B}$) is reversed.

The Zeeman components selected for observa-

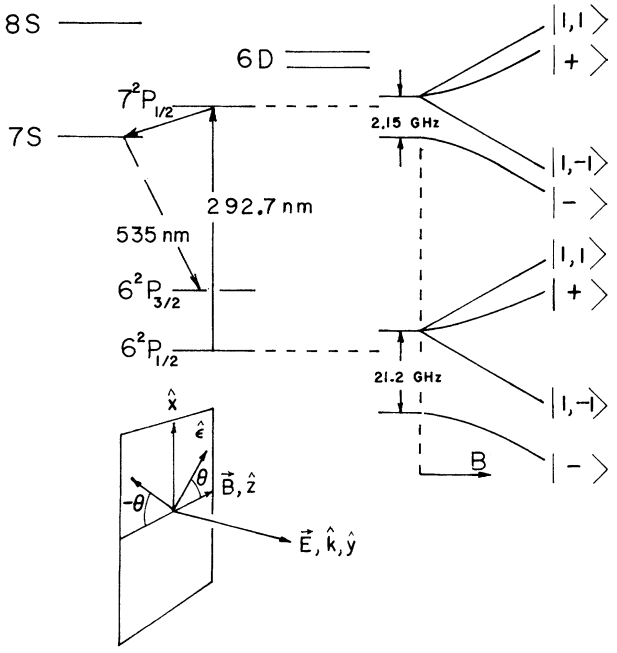

FIG. 1. Experimental coordinate system and low-lying energy levels of Tl (not to scale) showing hyperfine and Zeeman splittings of $6P$ and $7P$ states. States not mixed by the magnetic field are labeled $|F,m_F\rangle$. States labeled $|\pm\rangle$ are those for which $m_J = \pm\frac{1}{2}$, respectively, in the limit of large B.

tion are

$$\left.\begin{array}{l} 6^2P_{1/2} \rightarrow 7^2P_{1/2} \\ |1,-1\rangle \rightarrow |1,-1\rangle \\ |1,1\rangle \rightarrow |1,1\rangle \end{array}\right\} \Delta m_F = 0 \qquad (1)$$

$$|1,-1\rangle \rightarrow |+\rangle \quad \Delta m_F = 1.$$

At the peak of the resonance dominated by $|1,-1\rangle \rightarrow |1,-1\rangle$, $|1,1\rangle \rightarrow |1,1\rangle$ (which occur at the same frequency) there is some overlap of $|+\rangle \rightarrow |+\rangle$. Separated by 2.2 GHz is an adjacent peak containing mainly $|1,-1\rangle \rightarrow |+\rangle$ but with some overlap of $|+\rangle \rightarrow |1,1\rangle$ (see Fig. 2). The transition probabilities for the two resonances indicated in Eq. (1) are

$$T_{\Delta m_F=0} \propto [\beta^2 E^2 \sin^2\theta - 2\beta E \,\mathrm{Im}\,\mathscr{E}_p \sin\theta\cos\theta],$$
$$T_{\Delta m_F=1} \propto [\beta^2 E^2 \cos^2\theta + 2\beta E \,\mathrm{Im}\,\mathscr{E}_p \sin\theta\cos\theta]. \qquad (2)$$

In general $\Delta m_F = 0$ and $\Delta m_F = \pm 1$ lines contribute interference terms of opposite sign and $B = 3.2$ kG is chosen to minimize overlap of nearby Doppler broadened lines. We choose $\theta = \pm 35°$ so that the signal sizes on the two transitions in (2) are equal. The interference term, $2\beta E \,\mathrm{Im}\,\mathscr{E}_p \sin\theta\cos\theta$, is extracted by looking for an asymmetry:

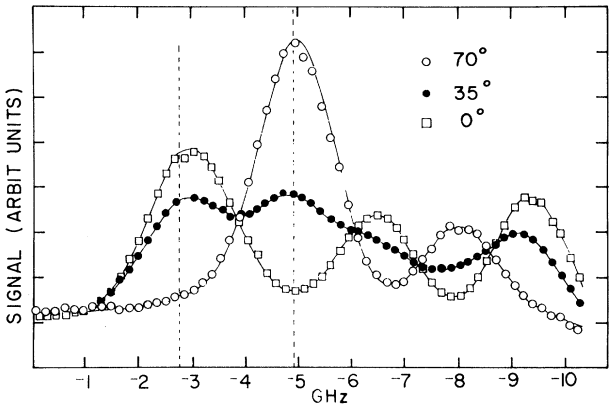

FIG. 2. Laser scan of $6^2P_{1/2}$, $F=1 \rightarrow 7^2P_{1/2}$, $F=1$ hyperfine structure for $B = 3.2$ kG, $\theta = 0°$, 35°, 70°. The solid curves are theoretical. The dashed vertical lines indicate where parity data are taken ($\Delta m_F = 0$: -4.9 GHz; $\Delta m_F = 1$: -2.7 GHz).

$$\Delta = \frac{T(+)-T(-)}{T(+)+T(-)} = \begin{cases} -\,\mathrm{Im}\dfrac{2\mathscr{E}_p}{\beta E}\cot\theta, & \Delta m_F = 0 \\ +\,\mathrm{Im}\dfrac{2\mathscr{E}_p}{\beta E}\tan\theta, & \Delta m_F = \pm 1, \end{cases} \qquad (3)$$

where $T(\pm)$ refers to the transition probability (as measured by 535-nm intensity) for two coordinate systems of opposite parity defined by the relative orientations of $\hat{\epsilon}$, $\vec{E}$, and $\vec{B}$.

A Nd-doped yttrium aluminum garnet–pumped dye laser oscillator-amplifier system described in detail elsewhere[9] generates 5-nsec, 3-MW pulses of 585-nm light in a bandwidth of ~ 100 MHz with a repetition rate of 17 Hz. This passes unfocused through a deuterated potassium dihydrogen phosphate crystal to generate 293-nm light. The uv beam, linearly polarized along $\hat{z}$, then passes through two Pockels cells operating as half-wave plates, which can orient $\hat{\epsilon}$ at angles $\theta = 0°$, $\pm 35°$, or 70°. The quality of the linear polarization is checked periodically with a Glan air prism, and the extinction is typically 10^{-3}. The 293-nm beam (typically 2 mJ/pulse) then enters a vacuum chamber and passes through a quartz cell surrounded by an oven at 950 K. The cell contains Tl vapor (99.44% ^{205}Tl, 0.56% ^{203}Tl) with density 5×10^{14} cm^{-3}. There are two interaction regions in the cell, defined by nickel disk electrodes coaxial with the laser beam. The electric fields, known to $\pm 3\%$, are opposite in the two regions, while $\vec{B}$ and $\hat{\epsilon}$ are the same for both. The 535-nm fluorescence signal from each region is collimated by a lens, filtered, and refocused onto the photocathode of a photomultiplier tube. Typically, we collect about 10^5 photoelectrons in each tube per laser pulse. Each photomultiplier-tube signal is integrated, amplified, digitized, and stored in an LSI-11 computer which randomly changes the sign of $\vec{E}$ and θ on a pulse-to-pulse basis. The computer also controls the laser frequency and switches back and forth automatically between the $\Delta m_F = 0$ and $\Delta m_F = 1$ transitions of interest every 1024 laser pulses. The magnetic field is reversed after sixteen groups of 1024 pulses. In order to keep the laser on resonance the Pockels cell voltages are switched every sixteen pulses so there is one pulse of the laser with $\theta = 0°$ and one with $\theta = 70°$. As can be seen in Fig. 2, at 0° only the $\Delta m_F = \pm 1$ components are excited, whereas at 70° the $\Delta m_F = 0$ components are dominant. The maximum parity asymmetry occurs on the $\Delta m_F = 0$

line when the ratio, R, of the signal intensity at 70° to that at 0° is a maximum. The laser frequency is stabilized by means of an automatic feedback loop that maximizes R for $\Delta m_F = 0$ data. The frequency is then shifted a fixed amount to where R is a minimum for $\Delta m_F = 1$ data.

A PNC asymmetry is formed from the data by first computing an asymmetry for the two regions: $\Delta = (N_1 - N_2)/(N_1 + N_2)$. This normalizes out laser fluctuations. We then calculate $\Delta_{\rm PNC} = [\Delta^{++} - \Delta^{+-} - \Delta^{-+} + \Delta^{--}]/4$ where $+$, $-$, etc., refer to the configurations $E, \theta = ++, +-, -+, --$.

False asymmetries can arise from terms in the transition probability with the same signature as PNC (odd under reversal of $\vec{\mathrm{E}}$, θ; even under reversal of $\vec{\mathrm{B}}$). Such terms result from misalignment of $\vec{\mathrm{E}}$ and $\vec{\mathrm{B}}$ and imperfections in their reversal, as well as from imperfect linear polarization of laser light. Each of these effects is determined by direct measurements of the undesired and nonreversing components of $\vec{\mathrm{E}}$ and $\vec{\mathrm{B}}$, and the imperfections in $\hat{\epsilon}$. Some are determined simultaneously with parity data, and some are measured in independent experiments using circular polarization of the 293-nm light, mechanical rotation of the vacuum chamber, cell, and laser beam relative to $\vec{\mathrm{B}}$, and other techniques. These auxiliary experiments and analysis of the systemtatics will be described in detail in a separate publication. Typically the off-axis components of $\vec{\mathrm{E}}$ and $\vec{\mathrm{B}}$ are measured to be a few parts in 10^3 while the nonreversing components of $\vec{\mathrm{E}}$ are a few parts in 10^4. The total measured contribution of all the systematic terms is very small:

$$\Delta^{\rm false}(\Delta m_F = 0) = (-15 \pm 14) \times 10^{-7},$$
$$\Delta^{\rm false}(\Delta m_F = 1) = (+5 \pm 14) \times 10^{-7}. \quad (4)$$

A total of 1.2×10^7 laser pulses of PNC data were accumulated, equally divided between the two Zeeman components. Four values of electric field were employed: $E = 67$, 109, 188, and 351 V/cm. Figure 3(a) shows the average asymmetry $\bar{\Delta} = \frac{1}{2} \times [\Delta(\Delta m_F = 0) - \Delta(\Delta m_F = 1)]$ for the two Zeeman components plotted versus $1/E$. These data have been corrected for systematic effects [Eqs. (4)], line overlap dilution, and $\cot\theta$, $\tan\theta$ factors, and for finite signal-to-background ratio. Of these, only the last varies with E. The observed asymmetry is proportional to $1/E$, as expected. In Fig. 3(b) we plot the asymmetry for each Zeeman component separately, where we have combined the data for all four electric fields together by assuming a $1/E$ dependence, after correcting for finite signal-to-background. As expected, the two asymmetries have opposite sign, and the relative magnitudes are consistent with a calculation of asymmetry as a function of frequency.

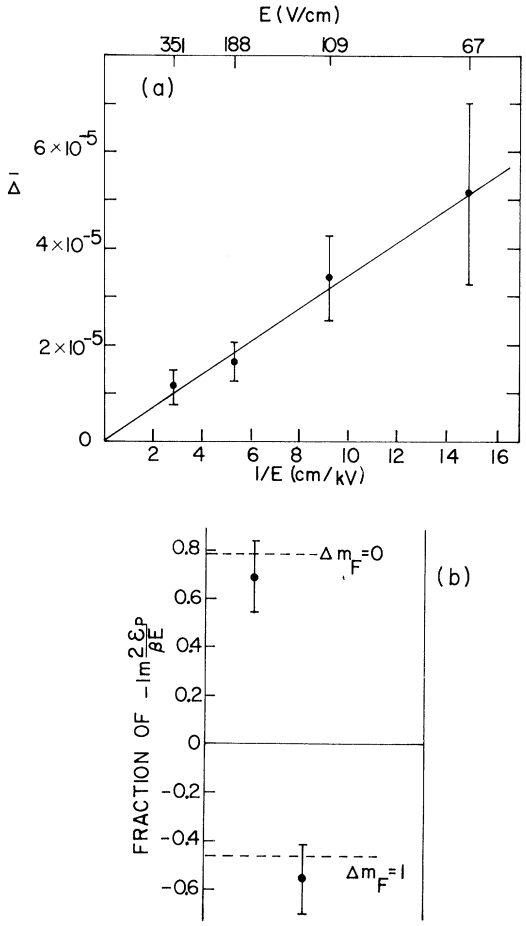

FIG. 3. (a) Average PNC asymmetry, $\bar{\Delta}$, for two Zeeman components vs $1/E$. The line is a least-squares fit to the data points (see text). It is not constrained to pass through the origin *a priori*. (b) Experimental asymmetry, Δ, for the two hyperfine components separately. The data from the different values of electric field have been combined assuming a $1/E$ dependence, and are plotted as the fraction of $-\mathrm{Im}2\mathscr{E}_p/\beta E$ measured on each transition. Dashed lines indicate the theoretical prediction for relative sizes of the asymmetry.

From the slope of the line in Fig. 3(a) we obtain

$$\mathrm{Im}[\mathscr{E}_p/\beta] = -1.73 \pm 0.26 \pm 0.07 \text{ mV/cm}, \quad (5)$$

where the first and second uncertainties are statistical and systematic, respectively. In Table I this result is compared with the previous experimental

TABLE I. Comparison of experimental and theoretical values for Im $\mathcal{E}_p/\beta$. Values of $\mathcal{E}_{p,\text{theor}}$ assume (Ref. 1) $Q_W = Z(1-4\sin^2\theta_W) - N$ with (Ref. 10) $\sin^2\theta_W = 0.215$. Reference 11 does not report a value for β. The value marked with an asterisk is obtained using β_{theor} quoted in text (Ref. 7).

$\text{Im}(\mathcal{E}_p/\beta)\|_{\text{expt.}}$ (mV/cm)	$\text{Im}(\mathcal{E}_p/\beta)\|_{\text{theor}}$ (mV/cm)	$\mathcal{E}_{p,\text{theor}}$	Ref.
-1.73 ± 0.33			This work
$-1.80^{+0.65}_{-0.60}$			Ref. 5
	-1.31 ± 0.26	$(-2.07 \pm 0.45) \times 10^{-8} \mu_0 i$	Ref. 7
	$-1.04 \pm 0.16^*$	$(-1.70 \pm 0.08) \times 10^{-8} \mu_0 i$	Ref. 11

result[5] and with two theoretical calculations[7,11] based on the $SU(2) \times U(1)$ electroweak model. The first of these[7] employed the one-electron–central-field approximation and ignored many-body effects. The second,[11] based on relativistic many-body perturbation theory, took into account electron-electron interaction terms and found them to be significant. A measurement of β now underway in our laboratory will enable us to determine $\mathcal{E}_p$ directly.

It is a pleasure to thank Steven Chu for his invaluable contributions to the laser system, and glassblower Dane Anderberg and machinist Frank Lopez for excellent workmanship. This work was supported in part by a National Science Foundation graduate fellowship and a Bell Telephone Laboratories grant through the Graduate Research Program for Women. This research was supported by the Director, Office of Energy Research, Office of Basic Energy Sciences, Chemical Sciences Division of the U. S. Department of Energy under Contract No. DE-AC03-76SF00098.

[1]M. A. Bouchiat and C. Bouchiat, Phys. Lett. **B48**, 111 (1974), and J. Phys. Paris **35**, 899 (1974), and **36**, 493 (1975).

[2]J. H. Hollister *et al.*, Phys. Rev. Lett. **46**, 643 (1981), and references therein.

[3]T. P. Emmons, J. M. Reeves, and E. N. Fortson, Phys. Rev. Lett. **51**, 2089 (1983).

[4]M. A. Bouchiat, J. Guena, L. Hunter, and L. Pottier, Phys. Lett. **B117**, 358 (1982), and **B134**, 463 (1984).

[5]P. H. Bucksbaum, E. D. Commins, and L. R. Hunter, Phys. Rev. D **24**, 1134 (1981).

[6]S. Chu, E. Commins, and R. Conti, Phys. Lett. **A60**, 96 (1977).

[7]D. Neuffer and E. D. Commins, Phys. Rev. A **16**, 844 (1977).

[8]This method was proposed independently by M. A. Bouchiat, M. Poirier, and C. Bouchiat, J. Phys. Paris **40**, 1127 (1979), and by E. Commins [see P. H. Bucksbaum, in Proceedings of the Workshop on Parity Violation in Atoms, Cargèse, Corsica, 1979 (unpublished)].

[9]P. Drell and S. Chu, Opt. Commun. **28**, 343 (1979).

[10]B. P. Das *et al.*, Phys. Rev. Lett. **49**, 32 (1982).

[11]W. J. Marciano and A. Sirlin, Phys. Rev. D **27**, 552 (1983).